Quaternary International 408 (2016) 78–92

Contents lists available at ScienceDirect

Quaternary International

journal homepage: www.elsevier.com/locate/quaint

Differential impact of long-shore currents on coastal geomorphology development in the context of rapid sea level changes: The case of the Old Sefidrud (Caspian Sea)

Safiyeh Haghani*, Suzanne A.G. Leroy

Environmental Science, Brunel University London, London UB8 3PH, UK

ARTICLE INFO

Article history:
Available online 21 January 2016

Keywords:
Coastal lagoons
Caspian Sea
Rapid sea level rise
Geomorphological changes
Little Ice Age

ABSTRACT

In the face of global rise in sea level, understanding the response of the shoreline to sea level rise is an important key for coastal management. The rapid sea level fluctuations taking place in the Caspian Sea provide a live model for studying shoreline response to sea level rise. Coastal lagoon deposits provide an ideal archive to study sea level fluctuation. In this study, two lagoons on both sides of the Old Sefidrud River (south coast of the Caspian Sea) have been subjected to study using sedimentology, palynology and macro-remains analyses: the Amirkola and the Klaus Lagoons. The results demonstrate how these coastal lagoons, related to one single river within the same delta, during the last decades respond differently to sea level fluctuations and show the crucial role played by long-shore current.

1. Introduction

The Caspian Sea (CS) is the largest lake in the world (surface area of 371,000 km^2). It is well known for its large fluctuation of the water levels: during the 20th century it has experienced a ~3 m fall and rise (Fig. 1A), while the global sea level has fluctuated approximately 2 mm/y in the same period (Kroonenberg et al., 2007). Coastal geomorphology has undergone rapid and varied changes in response to water level changes including passive inundation, beach–ridge formation, barrier–lagoon development and common coastal erosion (Kaplin and Selivanov, 1995; Naderi Beni et al., 2013a). On the southwestern CS coast of Iran, major geomorphological changes occurred in the east of the Sefidrud Delta where the Old Sefidrud delta is located (Fig. 1B). The Sefidrud avulsed several times during the Holocene, and the last major avulsion occurred when the river diverted its course from the Amirkola Lagoon area in the east to the Kiashahr Lagoon area in the west some 400 years ago (Kousari, 1986; Krasnozhon et al., 1999; Lahijani et al., 2009; Leroy et al., 2011; Kazancı and Gulbabazadeh, 2013; Naderi Beni et al., 2013b). The pre-avulsion river is known as Old Sefidrud. Holocene lagoonal deposits around the old-Sefidrud delta comprise of coastal geomorphological response to sea level change and delta-avulsion. This paper discusses sea level change for the Caspian Sea, although the CS is strictly a lake. This multidisciplinary study focuses especially on the Amirkola Lagoon (located east of the Old Sefidrud) and a newly discovered lagoon, i.e. Klaus Lagoon (west of the Old Sefidrud) (Fig. 1B). We aim to investigate the impact of rapid CS level fluctuations on coastal geomorphology and vegetation.

2. Study area

2.1. Caspian Sea

During the last millennium, CS level experienced two significant changes: a poorly identified drop in the early medieval period and a slightly better known rise at the end of the Medieval Climatic Anomaly (MCA, AD 950–1250) and a clear highstand in the Little Ice Age (LIA, AD 1350–1850) (dates defining these periods from Kroonenberg et al., 2007; Ruddiman, 2008; Mann et al., 2009: Leroy et al., 2011; Naderi Beni et al., 2013a; Haghani et al., 2015). During the 20th century, the CS has experienced a ~3 m fall and rise. After the water levels peaked in 1995, at −26.24 m bsl, levels have been dropping slightly (at −27.41 m bsl, in 2014).

Inundation, erosion and sand barrier and back-barrier lagoon formation are the main responses of the coastal area to rapid water level rise (Kaplin and Selivanov, 1995; Kroonenberg et al., 2000;

* Corresponding author.
E-mail address: Safiyeh.Haghani@gmail.com (S. Haghani).

http://dx.doi.org/10.1016/j.quaint.2015.11.127

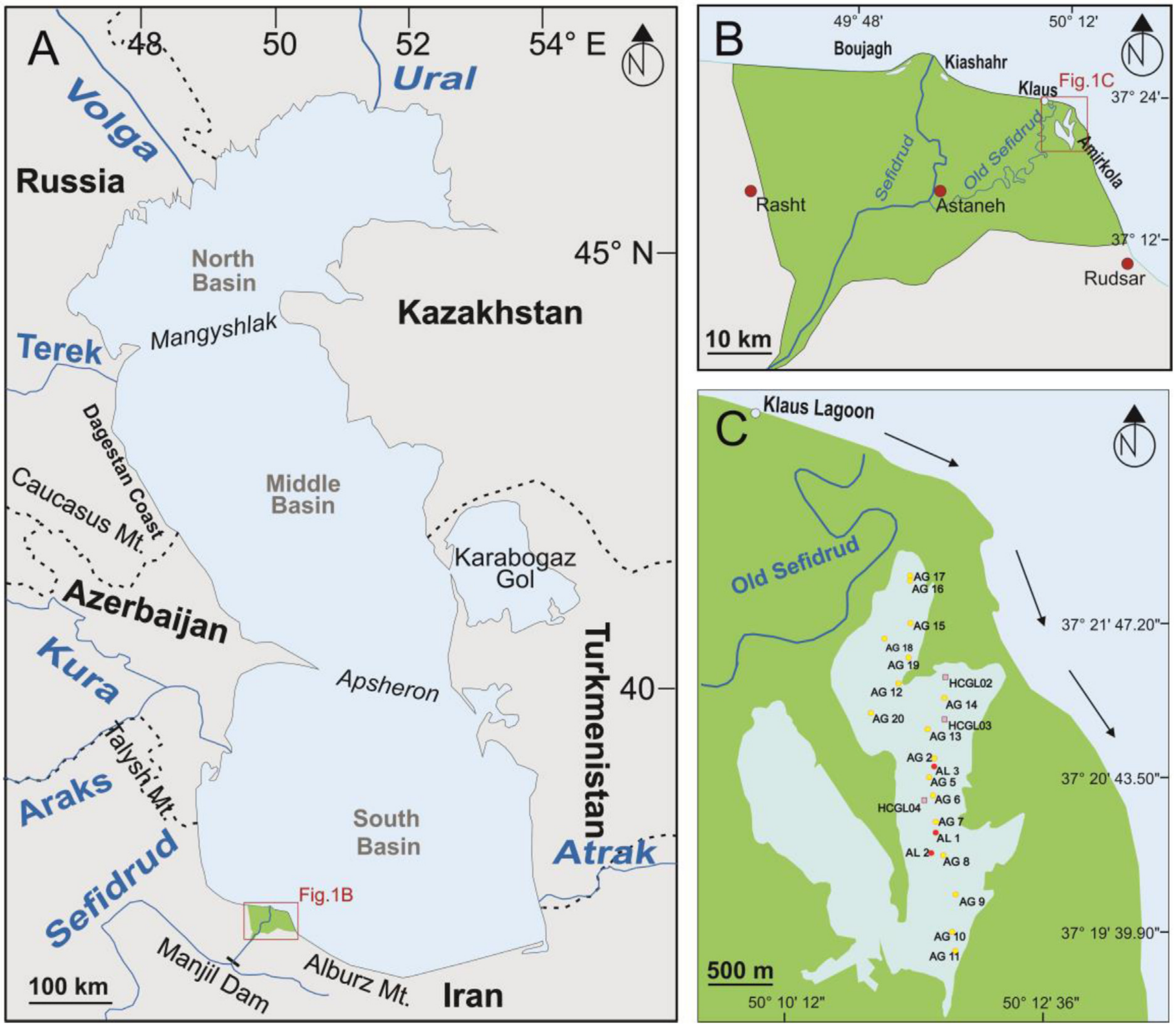

Fig. 1. A: Location map of the Caspian and major rivers flowing to the Caspian Sea. Black dashed lines: international boundaries, Mt.: Mountains, B: Location of Amirkola and Klaus Lagoons within the Sefidrud Delta. Red dots: location of important towns, C: Location of the cores taken from Amirkola Lagoon. Core identification has been simplified in this map, i.e.: AG17 full identification is AL11G17. Red dots represent the location of core taken by Livingstone corer and yellow dots the location of cores taken by gravity corer. Pink squares show location of cores in Leroy et al. (2011). Black arrows show the direction of longshore currents.

Naderi Beni et al., 2013b). The CS level rise between 1979 and 1995 affected deltas by inundation and erosion. Kroonenberg et al. (2000) showed that this period was characterised by erosion and development of sand barrier and lagoons behind them in Dagestan Coast (western coast of the middle CS). Sand barriers can also be formed during water level fall as small bars without lagoon development (Kroonenberg et al., 2000). During such a period of fall, existing lagoons also became shallower and narrower (Kroonenberg et al., 2000) and some changed to marshland (Kaplin et al., 2010). Human activities such as reduction of sediments by dam construction may cause intensive erosion of coasts and deltas (Ignatov et al., 1993; Lahijani et al., 2008) by sediment starvation.

2.2. Lagoon setting

The Sefidrud has repeatedly changed its course through the area between the Anzali and Amirkola lagoons (Kousari, 1986). The last major avulsion occurred some 400 years ago when the river diverted its course from the east, near Amirkola Lagoon, towards the west near Kiashahr Lagoon, shifting its outlet ~23 km westwards (Krasnozhon et al., 1999; Lahijani et al., 2009; Leroy et al., 2011; Kazancı and Gulbabazadeh, 2013; Naderi Beni et al., 2013b).

The Amirkola Lagoon is associated with the Old Sefidrud and has a maximum water depth of 2 m (Naderi Beni et al., 2013b). The lagoon has no river inflow and receives freshwater by precipitation and surface water passing through rice fields that surround the lagoon. Lahijani et al. (2009) studied the coastal evolution of the Sefidrud Delta including lagoon development in the area. The authors suggested that the Amirkola Lagoon was formed by littoral drift of sediments supplied by the Old Sefidrud, during the Little Ice Age (LIA: around 1600 AD), as a result of CS level rise. Naderi Beni et al. (2013b) studied the area around the Amirkola Lagoon using Ground Penetrating Radar (GPR) profiles and concluded that the development of this lagoon was a response to rapid CS level rise during the LIA, but age confirmation was lacking. Leroy et al. (2011) conducted a palynological study on Amirkola Lagoon cores. Their investigation shows that Amirkola Lagoon was under CS level influence during the Late LIA and became isolated from the CS after the high stand. A radiocarbon dating provided in their study shows a calibrated radiocarbon age of AD 1750 for the lagoon and the authors estimated the initiation to have occurred around AD 1700.

During a field campaign in 2011, the remains of an old lagoon in the west of the Sefidrud were discovered by Dr Klaus Arpe in a beach outcrop that is being eroded during storm surges (Fig. 1 B and C). This lagoon has not been studied before and is named here after its discoverer: Klaus Lagoon. This lagoon was investigated in an outcrop from which the cored sedimentary sequence AL11V3 was obtained.

2.3. Climate, geology, vegetation

The Amirkola and Klaus lagoons are located in an area with a temperate humid climate and high precipitation. Annual precipitation in the study area is ~1450 mm, with 77.2% mean humidity, and mean annual temperature is ~16 °C (Lahijan meteorological station: Molavi–Arabshahi et al., 2015). The study area is a coastal lowland situated at the foot of the central Elburz Mountains. The coastal plain contains various active river and delta systems characterized by abundant distributary channels and wide flood plains. Caspian Sea deposits are locally found on the coastal plain, reflecting its formation under past sea level high stands (Lahijani et al., 2008). The vegetation in the area of Amirkola is dominated by *Phragmites* reedbeds with diverse aquatic plants (Fig. 2 in Leroy et al., 2011). On the shores, a dense alder swamp occurs. The area of Klaus Lagoon outcrop is a mixture of undeveloped wasteland and field and rice paddies (Fig. 2 in Leroy et al., 2011).

3. Materials and methods

3.1. Sediment coring

Twenty one sediment cores with a maximum composite depth of 119 cm were obtained using a gravity corer and a Livingstone corer during the field campaign organised with the Iranian National Institute for Oceanography and Atmospheric Science (INIOAS) in 2011 from Amirkola Lagoon (Fig. 1C).

A sequence with a composite depth of 281 cm was cored in the Klaus Lagoon deposits using a percussion corer from the top of an outcrop along the beach (Fig. 1 B and C). The accurate elevation of the outcrop (AL11V3) on a west–east section of the coast, west of the Sefidrud mouth, was surveyed 29 months after the coring campaign, by INIOAS using a Leica Sprinter 150M Electronic Level in relation to a bench mark in Dastak town. The outcrop had meanwhile eroded further inland, especially during storms. Therefore, a key layer was chosen to link the observations between 2011 and 2014 and sampling at these different times. A conspicuous red layer in the outcrop was considered as the key marker layer.

3.2. Sedimentology

Magnetic susceptibility (MS) measurements were performed on all the cores using a Bartington MS2C core logging sensor at a 2 cm interval. MS in this study was used to propose an intra-lagoonal correlation between the cores and also as an indicator of depositional sedimentary environment.

A standard visual core description was performed immediately after core photography (Mazzullo et al., 1988). Sediment colour was determined using a Munsell Colour Chart. Grain size and Loss-On-Ignition (LOI) analyses were performed on the sequences Al11G5 and AL11L2, in Amirkola Lagoon and on the single sequence in Klaus Lagoon, i.e. AL11V3. Grain size was determined using a CILAS 1180 particle size analyser on homogenised and representative subsamples. Soaking the samples in 10% tetra–sodium pyrophosphate solution and 20 s of ultrasound were used to prevent flocculation. Granulometric data were processed using the GRADISTAT program (Blott and Pye, 2001). The sand–silt–clay triangular diagram proposed by Folk (1974) was used for naming the textural group of the sediments. In addition, the particle size results of the sequence (Klaus Lagoon) have been presented in a 3D plot using

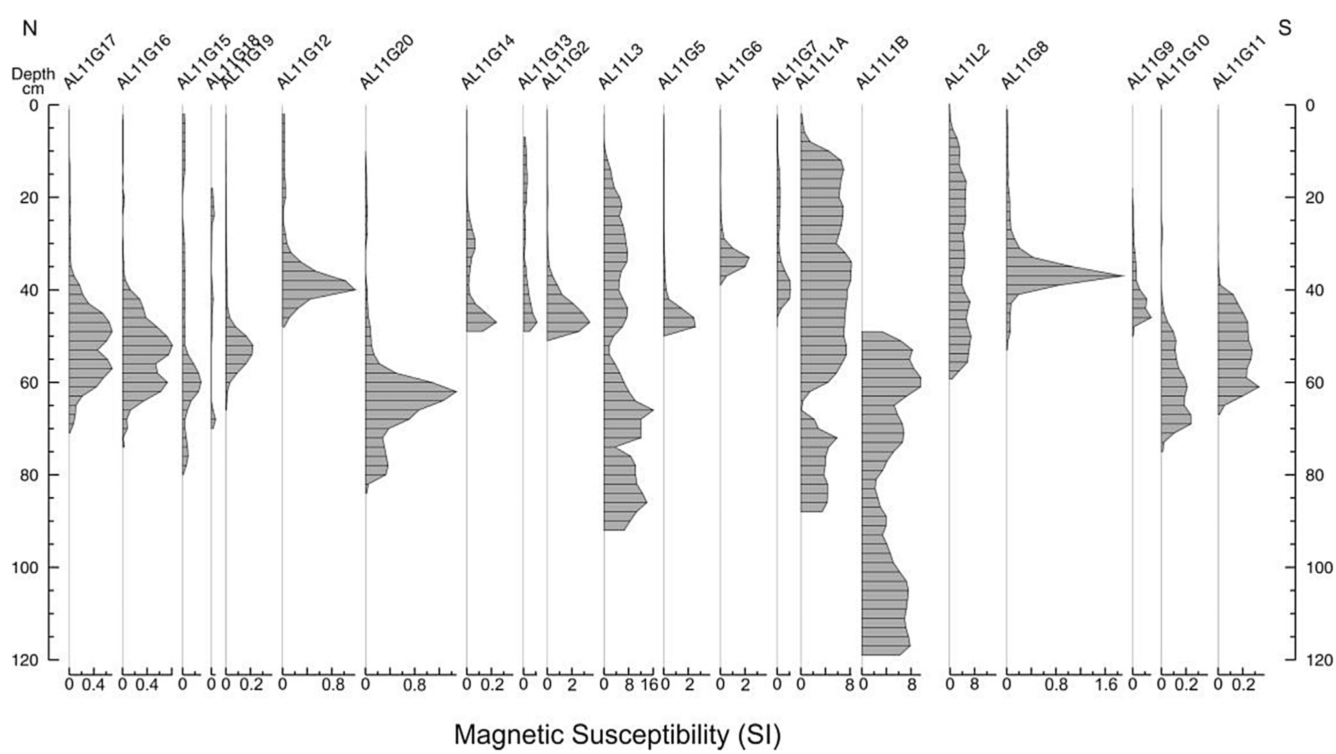

Fig. 2. Magnetic susceptibility values of cores taken from Amirkola Lagoon. Cores in the diagram are arranged from the north (left) to the south (right) of the lagoon.

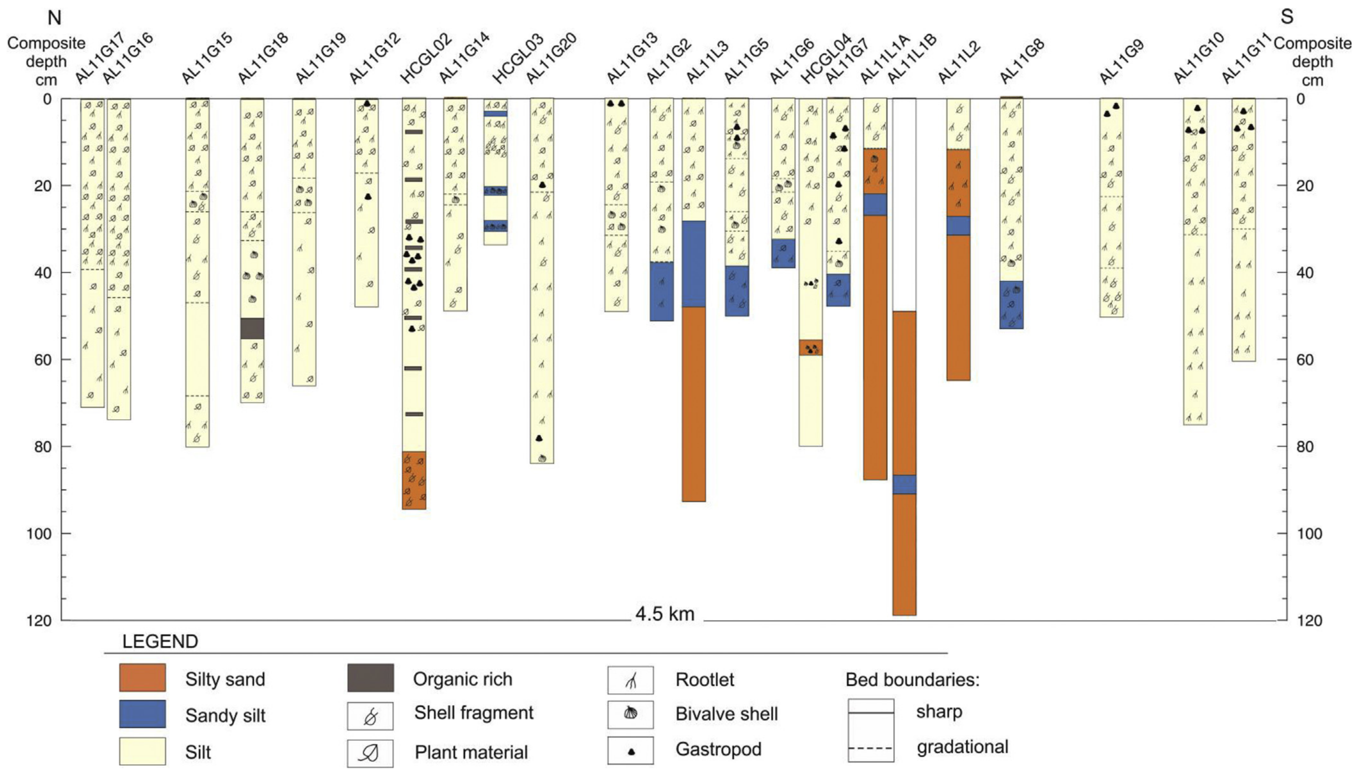

Fig. 3. Sedimentological logs of the cores from the Amirkola Lagoon. The logs have been arranged from the North to the South of the lagoon. Cores HCGL02, HCGL03 and HCGL04 from Leroy et al. (2011).

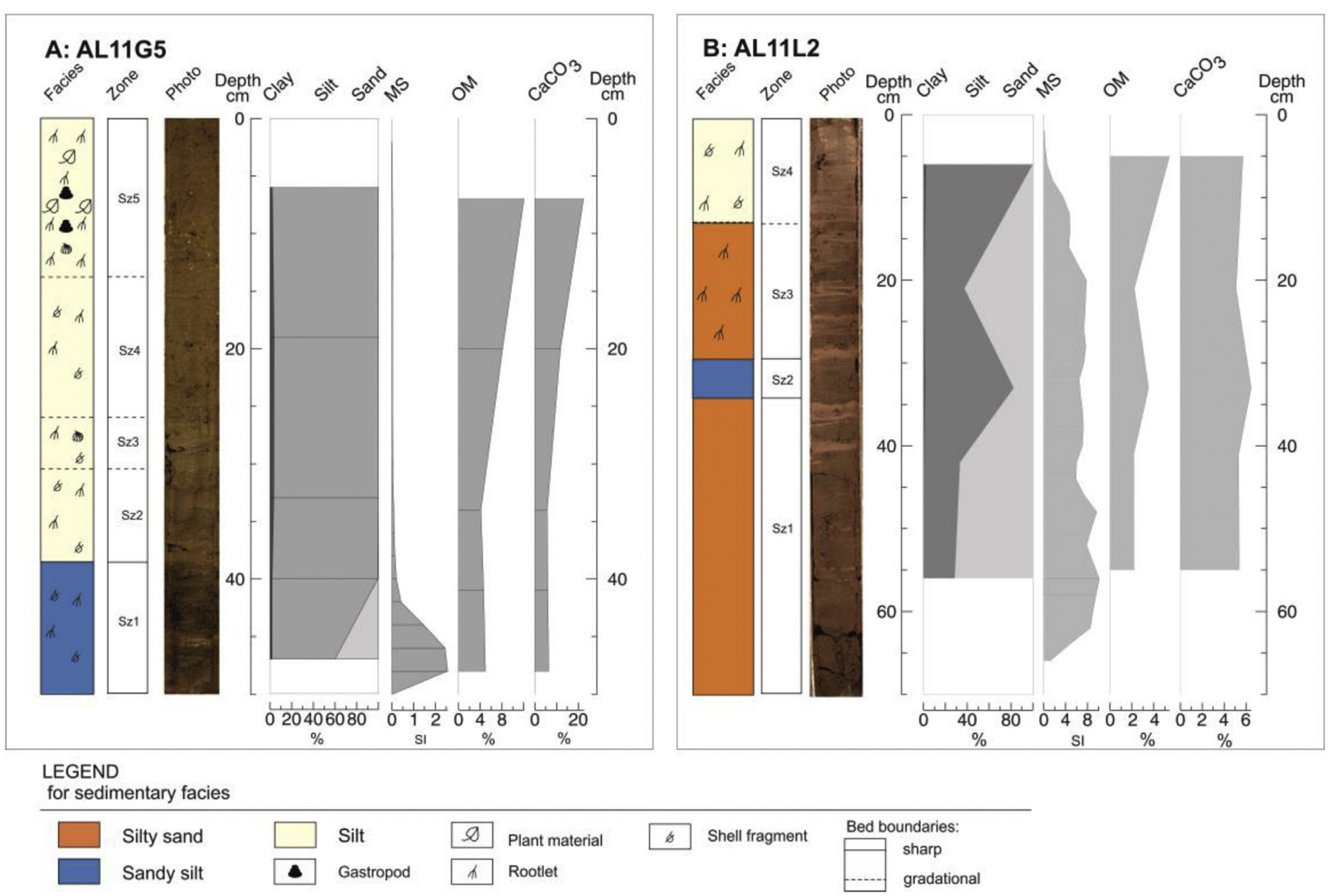

Fig. 4. A: Sedimentary log for core AL11G5, B: Sedimentary log for core AL11L2, displaying sedimentology, core photograph, grain size (clay, silt and sand), magnetic susceptibility (MS), organic matter (OM) and calcium carbonate ($CaCO_3$).

MATLAB software version 7.1 to highlight detailed changes over depth. Organic matter (OM) and calcium carbonate ($CaCO_3$) were determined through LOI, by burning the sample at 550 and 950 °C, respectively (Heiri et al., 2001).

3.3. Macro–remains

Twelve samples from the Klaus Lagoon sequence were selected to study macro-remains. Following the method of Birks (2001), samples with a weight of 15–20 g were deflocculated using 10% tetra–sodium pyrophosphate solution. The samples were then washed through a column of sieves with mesh diameters of 500, 125 and 53 μm. The finest fraction (53 μm) was used to retrieve microfossils such as foraminifers (Leroy et al., 2013). The residue was studied using a stereo–microscope (magnifications up to ×90). The samples above 500 and 125 μm were counted; the finest fraction was only scanned. The results are presented in percentage and concentration diagrams using the Psimpoll software, version 4.27 (Bennett, 2007). A zonation by CONISS after square–root transformation of the percentage data was applied.

3.4. Palynology

New palynological analyses were applied to the cored sequence of the Klaus Lagoon. Eleven sediment samples with a volume of 0.5–1.5 ml were soaked in 10% tetra–sodium pyrophosphate solution for deflocculation. The samples were then treated with cold HCl (first at 10% and then pure), cold HF (32%), followed by a repeated cold HCl treatment, in order to eliminate carbonates, quartz and fluorosilicate gels, respectively. Finally, the samples were sieved through 125 and 10 μm nylon meshes. The residues were mounted on glass slides in glycerol. The initial addition of *Lycopodium* tablets allowed the estimation of concentrations (number of palynomorphs per ml of wet sediment). Two samples were barren: i.e. at 101 and 86 cm depth.

A light microscope at ×400 magnification and at ×1000 for special identifications was used to count the palynomorphs. Pollen atlas and the reference collection at Brunel University London were used to identify the spores and pollen grains. Dinocysts were identified using the studies of Marret et al. (2004), Leroy et al. (2006), and Leroy (2010). Percentages of pollen, non-pollen palynomorphs and dinocysts were calculated on the sum of land–derived pollen (or terrestrial) only, with a median of 308 terrestrial pollen grains for the core samples. A zonation by cluster analysis (CONISS) after square–root transformation of the percentage data was applied to the main terrestrial taxa of the core samples.

3.5. Chronology

Two radiocarbon dates were obtained on plant remains from the Klaus Lagoon sequence at the Chrono Centre, Queen's University of Belfast, UK. Radiocarbon ages were calibrated using the CALIB programme version 7.1 (Stuiver and Reimer, 1993) with the IntCal13 calibration curve (Reimer et al., 2013).

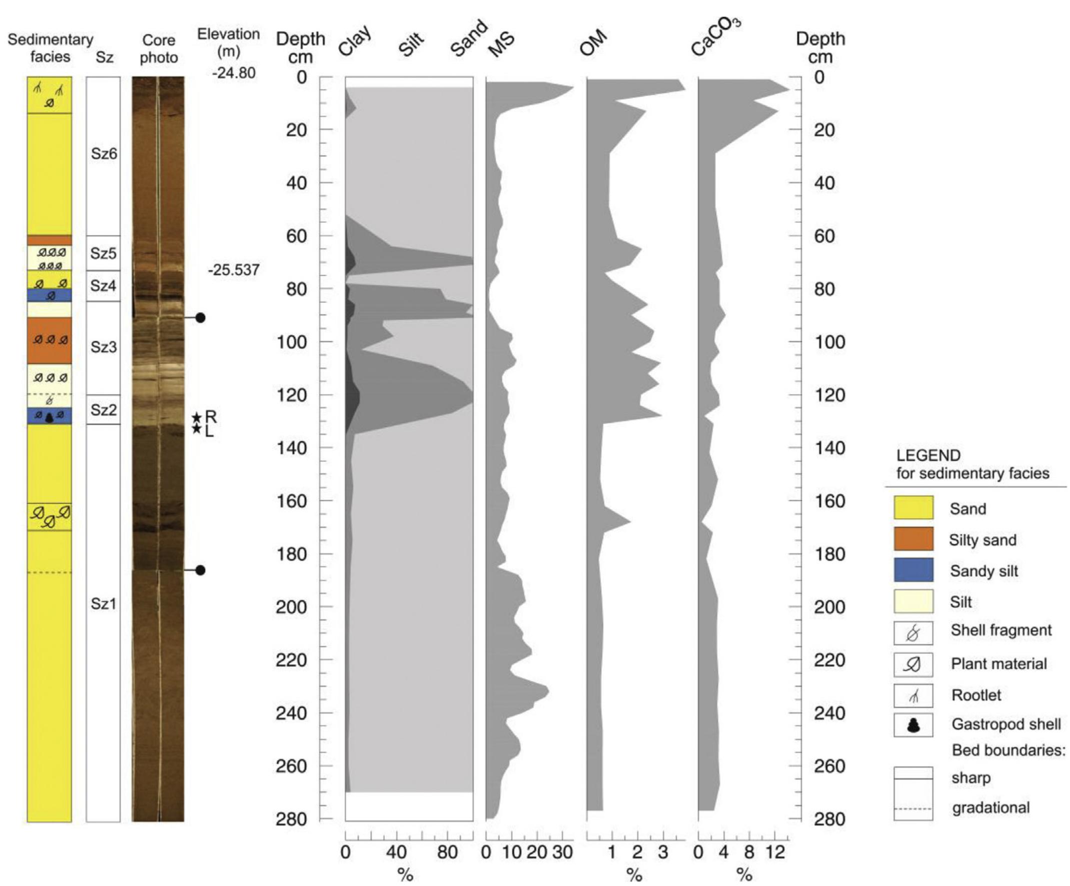

Fig. 5. Sedimentary log for the AL11V3 sequence (Klaus Lagoon), displaying sedimentology (Sz: sedimentological zone), core photo, grain size (clay, silt and sand), magnetic susceptibility (MS), organic matter (OM) and calcium carbonate ($CaCO_3$). Black stars refer to the depth of the radiocarbon dates, R: rootlets and L: leaf (material dated), and black pin symbols shows the core section limits.

4. Results

4.1. Amirkola Lagoon

The Magnetic Susceptibility (MS) shows strong variation along the cores (Fig. 2). In general, the base of the cores contains higher MS values, strongly dropping upward. The MS values of the cores located in the middle of lagoon (AL11G2 to AL11G8) are higher (up to 16) compared to those from marginal areas. The Amirkola Lagoon infill consists of clearly distinct sediment layers. From the bottom to the top, these layers contain: brown silty sand that appears at the base of the long cores in the middle of the lagoon (e.g. AL11L3, AL11L1 and Al11L2). This is overlain by a dark greyish brown sandy silt layer that in turn is covered by olive grey and olive brown silt. The olive grey silt interval contains *Theodoxus pallasi* shells which have been observed in the cores: AL11G15 (22 cm depth), AL11G18 (36–48 cm), AL11G19 (17–26 cm), AL11G14 (22 cm), AL11G20 (34–37 cm), AL11G2 (19 and 30 cm), AL11G5 (31–26 cm), AL11G6 (20–23 cm) and AL11G7 (35–40 cm). Furthermore, *Cerastoderma glaucum* was observed in the sandy silt layer in core AL11G8 and in the silty sand interval in the core AL11L1A. A very dark greyish brown silt layer was observed at the top of the cores, containing abundant plant material, rootlets as well as gastropods (Fig. 3).

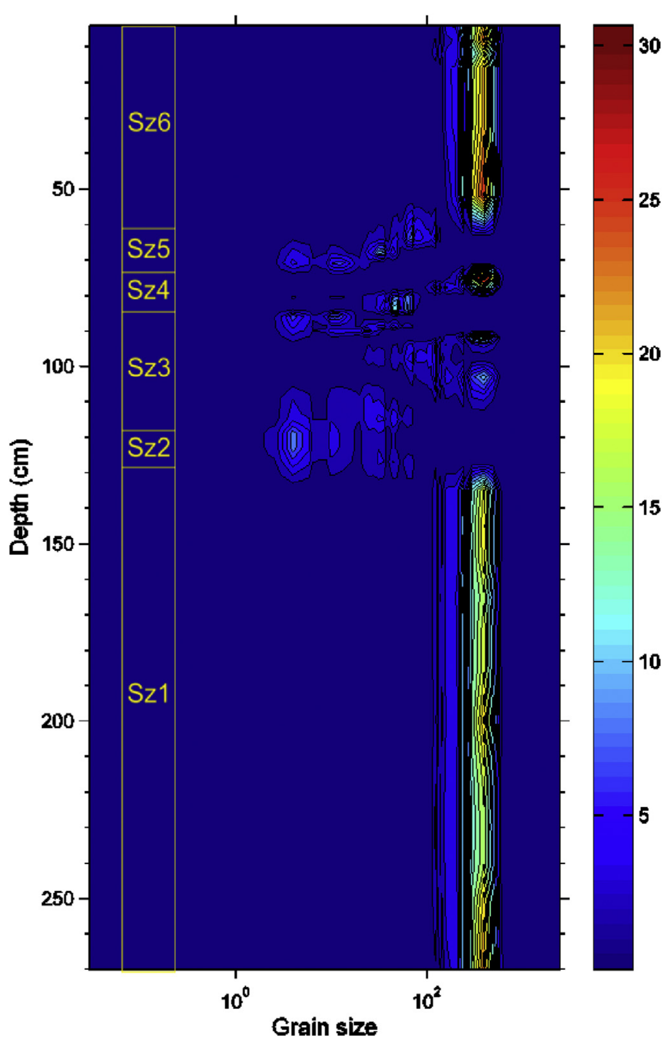

Fig. 6. 3D plot of grain size data in μm for the sequence AL11V3 (Klaus Lagoon): the dark blue colour represents the lowest volume (%), while the red colour shows the highest volume (%). Sz: sedimentological zone.

Cores AL11G5 and AL11L2 were selected for further study and are described in detail (Fig. 4).

Core AL11G5 is subdivided in five lithological units, from bottom to top:

Sz1, 50–38 cm: dark greyish brown sandy silt with bivalve fragments and rootlets.
Sz2, 38–31 cm: olive brown silt with shell fragments and rootlets. The lower contact is sharp.
Sz3, 31–26 cm: olive grey silt with *T. pallasi*, shell fragments and rootlets; Sz3 has a gradual lower contact
Sz4, 26–14 cm: olive brown silt with shell fragments and rootlets overlying gradually Sz3.
Sz5, 14–0 cm: very dark greyish brown silt with a considerable amount of plant material and rootlets, a *T. pallasi* at a depth of 11 cm and an unidentified gastropod at a depth of 6–8 6 cm. Lower boundary gradual.

The AL11G5 sequence consists mainly of silt and sandy silt. MS values are high at the base of the core (Sz1) with a peak at 55 cm depth, and sharply decrease in Sz2 and overlying units. Organic matter and carbonate content increase upward.

The sedimentology of the core AL11L2 from the bottom to the top is:

Sz1, 65–32 cm: brown homogenous silty sand
Sz2, 32–27 cm: dark greyish brown homogenous sandy silt; sharp lower contact.
Sz3, 27–12 cm: brown silty sand with shell fragments and rootlets; sharp lower boundary.
Sz4, 12–0 cm: olive brown silt with shell fragments and rootlets; lower contact sharp.

Core AL 11L2 contains is dominated by silty sand, sandy silt and silt. The MS values slightly decrease towards the top of the sequence while organic contents increase. Carbonate content is stable with a maximum value of 6.2% at a depth of 34 cm (Fig. 4).

4.2. Klaus Lagoon sequence

4.2.1. Sedimentology

Based on the core description and grain size results, this sequence is divided in six zones that are from the bottom to the top (Fig. 5):

Sz1, 281–131 cm: very thickly bedded dark brown sand with a 10 cm thin organic rich layer at a depth of 170–160 cm.
Sz2, 131–119 cm: Alternation of olive sandy silt and olive-grey silt with a thinly laminated layer (1 mm-thick) of plant material at a depth of 129 cm and gastropod shells (*T. pallasi*) and bivalve shell fragments at a depth of 124 cm. The base of the unit is sharp.
Sz3, 119–85 cm: Alternation of light brown silt and light reddish-brown silty sand with layers of plant material at 113 and 99 cm. Sharp lower boundary.
Sz4, 85–73 cm: Alternation of brown sandy silt and dark brown sandy silt with plant material; lower boundary sharp.
Sz5, 73–60 cm: Alternation of reddish-brown sandy silt and silt with thinly laminated layers (1 mm) of plant material at 71.5 and 65 cm. This is the lithofacies used for correlating the cored outcrop and the outcrop for which elevation was measured. Lower boundary is sharp.
Sz6, 60–0 cm: dark yellowish brown sand with plant remains and rootlets at the top 14 cm (Fig. 5).

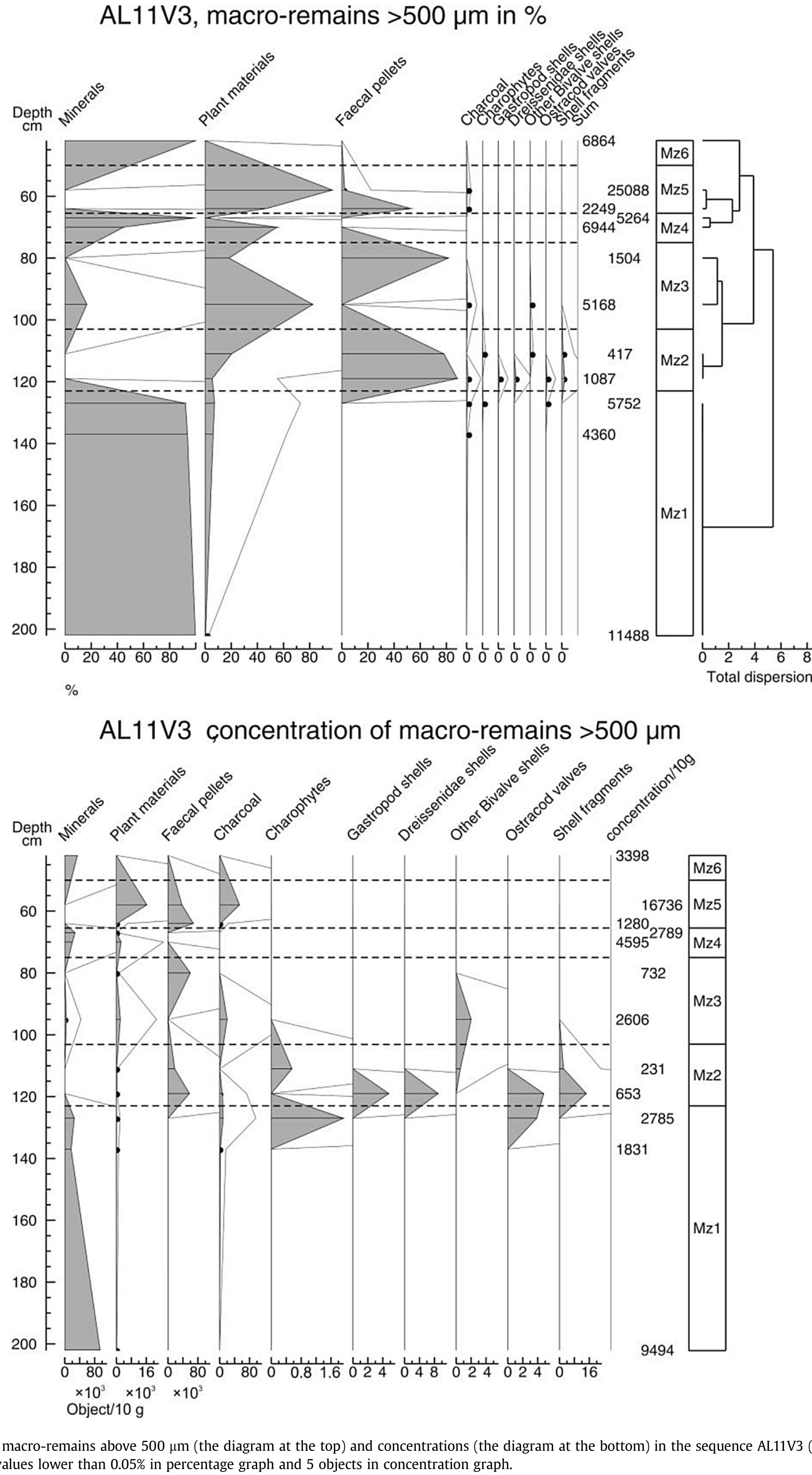

Fig. 7. Percentages of macro-remains above 500 μm (the diagram at the top) and concentrations (the diagram at the bottom) in the sequence AL11V3 (including Klaus Lagoon). Black dots represent values lower than 0.05% in percentage graph and 5 objects in concentration graph.

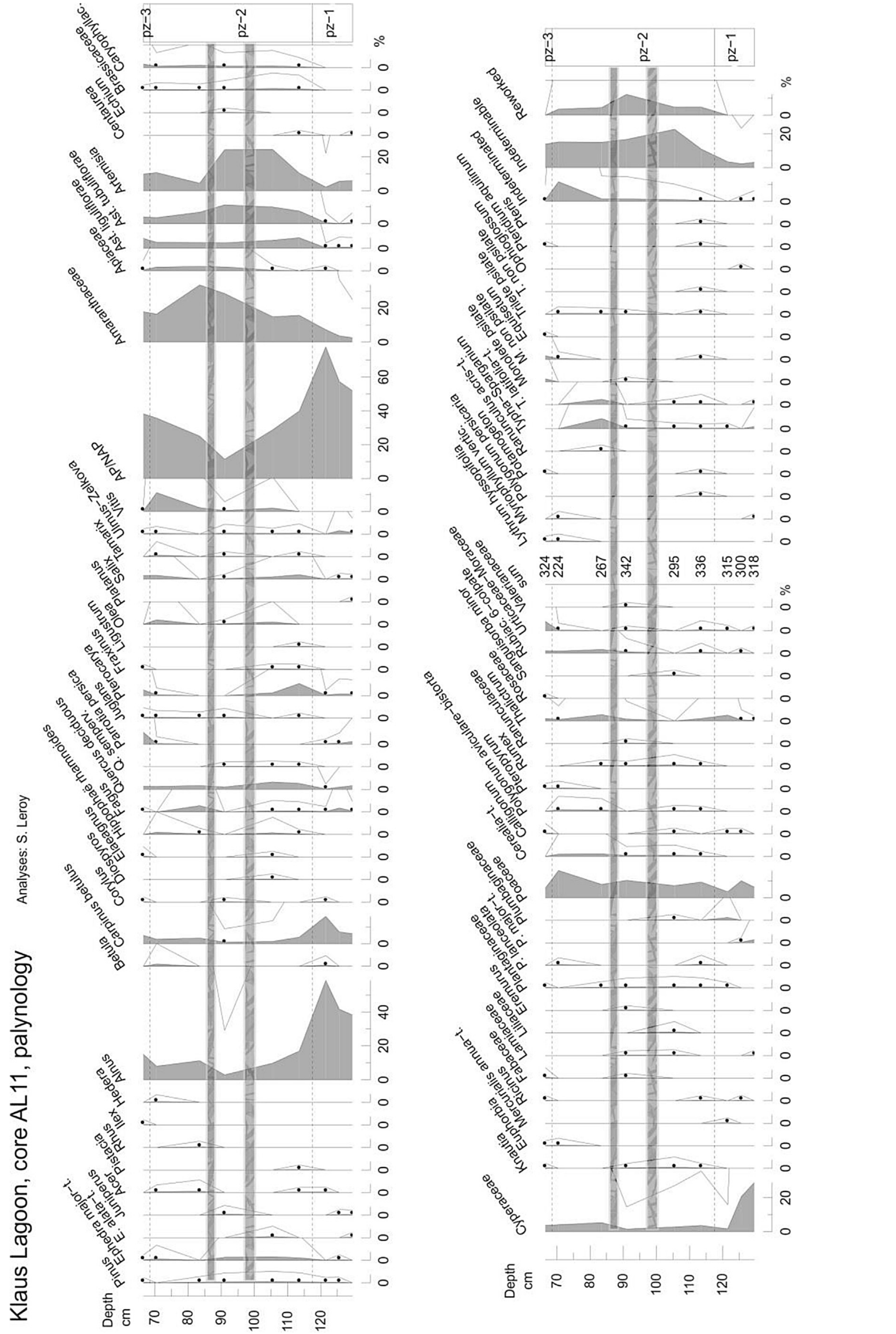

Fig. 8. Pollen, spores, non-pollen palynomorphs and dinocyst diagram for the Klaus Lagoon.

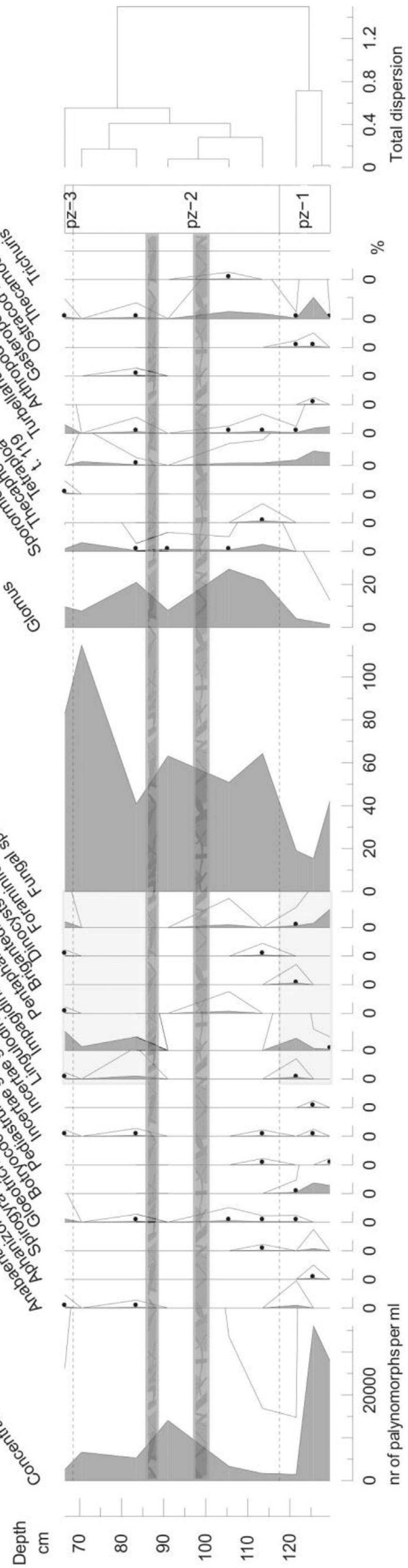

Fig. 8. (*continued*).

The elevation of the base of the red layer was −25.537 m. Taking into account the thickness of red layer, which is 73 cm, the elevation of the top of the outcrop is calculated at −24.80 m.

The 3-D graph of the grain size from 39 samples shows that the bottom and top of the sequence are mostly dominated by sand, with a maximum of 8% silt. The middle of the core (131–60 cm) mostly consists of silt with three peaks of sand (Figs. 5 and 6).

Overall, the bottom 98 cm of the sequence has relatively high MS values compared to the upper part. A peak of MS occurs at the top of sequence. From the base to 131 cm, the organic matter values are less than 1% with a small peak at a depth of 165 cm, followed by a sharp increase at a depth of 131 cm. From 131 to 60 cm, the OM is 2–3% and shows a continuous slight decrease upwards, with some fluctuations. Then it remained quasi constant from 60 to 14 cm, followed by a sharp increase in the top 14 cm. Overall, the carbonate content was constant along the sequence with two low points at the depths of 165 and 131 cm (corresponding to two peaks of OM), followed by a suddenly increase in the top 14 cm (Fig. 5).

4.2.2. Macro-remains

Ten different macro-remain types were identified in the fraction >500 μm and nine in the fraction >125 μm (Fig. 7 and Appendix A). Changes in macro-remains have been described based on the percentages of macro-remains at fraction 500 μm and meanwhile the main changes for the fraction of 125 μm (percentage and concentration) have been included in the above description. Based on the results, the sequence is divided into six zones suggested by the percentage of the 500 μm fraction.

Mz1, 204–123 cm (3 samples)

This zone is characterized by maximal values of minerals (92–100%) and <1–7% plant materials. A small amount of Charophytes (0.7%), charcoal (0.3%) and ostracod shells (0.1%) has been recognised at a depth of 128 cm. In the fraction of 125 μm, 98–100% minerals and 0–2% plant materials have been observed.

Mz2, 123–97 cm (2 samples)

This zone is dominated by the faecal pellets (78–88%) and plant materials (6–20%). Furthermore, 1–2% shell fragments, 1% Dressenidae (*Dreissena polymorpha*), <1% other bivalve species (larval shells), ~1% ostracod shells, ~1% gastropods (*Ecrobia grimmi* and *T. pallasi*), 1% charcoal and <1% charophytes have been recognised in this zone. Furthermore, 8%–80% minerals, 11–12% plant materials and 5–80% faecal pellets have been observed in the 125 μm fraction. Moreover, 3% Foraminifers (mainly *Ammonia beccarii* and some *Elphidiella brotzkajae*), <1% bivalve shells (in larval stage), 1% ostracod shells, <1% gastropod shells (broken *T. pallasi)* and <0.1% acari have been seen at a depth of 120 cm.

Mz3, 97–76 cm (2 samples)

The third zone is marked by a peak of faecal pellets (up to 82%), minerals (up to 17%) and plant materials (18–83%). Additionally, this zone contains a small amount of bivalve shells (larval shells) and charcoal (<1%). In the fraction of 125 μm, this zone is dominated by up to 97% minerals, up to 80% faecal pellets and 3–20% plant materials. Furthermore, <0.1% charcoal, 1% ostracods, <0.1% bivalve shells (larval) and <0.1% foraminifers (*A. beccarii* and *E. brotzkajae)* have been observed at a depth of 96 cm.

Mz4, 76–66 cm (2 samples)

The fourth zone is characterized by plant materials (<1–55%) and minerals (45–99%). The fraction 125 μm shows the same trend that includes 2–90% plant materials and 10 to 98 minerals.

Mz5, 66–51 cm (2 samples)

This zone is characterised by plant material (47–97%), faecal pellets (2–53%) and charcoal (<1%). The fraction of 125 μm is marked by minerals (28–59%), plant materials (40–54%) and faecal pellets (17%). Furthermore, less than 1% of charcoal, ostracod shells, bivalve shells (larval) and foraminifers (*A. beccarii* and *E. brotzkajae*) have been observed in this fraction.

Mz6, 51–42 cm (1 sample)

The sixth zone is distinct by 100% of minerals. In the fraction >125 μm, 1% plant materials and 99% minerals have been recognised at a depth of 43 cm.

4.2.3. Palynology

The preservation of palynomorphs is commonly compromised, as seen in the relatively high amounts of unidentifiable and reworked pollen grains. Three basal samples provide a well preserved spectrum. This is also reflected in concentrations that fluctuate around 5000 grains/ml, but that reach ~30,000 grains/ml in the two lowermost samples (129 and 126 cm).

In the arboreal pollen (AP), *Alnus* is generally dominant. A range of other deciduous trees is found: *Carpinus betulus*, *Quercus* and *Pterocarya*. In the NAP, Amaranthaceae and *Artemisia* are dominant, while Poaceae, Cyperaceae and other Asteraceae are present throughout. The aquatic pollen are scarce, but *Typha-Sparganium* and *Typha latifolia-t*. are present in low numbers throughout. In the NPP, some spores of freshwater algae, dinocysts and foraminifer inner organic lining occur. Fungal spores and especially *Glomus* are very abundant. Based on terrestrial pollen grains, three pollen zones have been identified including (Fig. 8):

Pz1, 130 to 117 cm

This zone contains a peak of *Alnus* (up to 59%) and of *Carpinus* (16%). The Cyperaceae are very high in the first sample (129 cm): 29%. *Botryococcus* is relatively abundant. Amaranthaceae increase slightly across this zone. The preservation and concentration are optimal for this sequence, although the concentrations sharply drop before the zone ends. Proportionally low fungal spores and *Glomus* occur. A mixture of freshwater algae and brackish organisms (dinocyst and foraminifers) is observed.

Pz2, 117 to 68 cm

This zone is still dominated by *Alnus*, albeit with much lower values (approx. 10%), and it starts with a small peak of *Pterocarya* and finishes with a small peak of *Vitis*. A maximum of *Artemisia* occurs first (24%), which is followed by a maximum of Amaranthaceae (34%). Poaceae are stable. Cerealia-t. appears, but is present in this zone only.

A sharp increase of indeterminable palynomorphs, reworked palynomorphs, fungal spores and *Glomus* is observed. Fungal spores reach a maximum at the end of this zone at 70 cm depth. Dinocysts and foraminifers are less abundant in this zone, except at 83 cm where the dinocyst *Impagidinium caspienense* increases slightly and briefly.

Pz3, 68 to 66 cm

This zone is made of only one sample at 66 cm. It is only distinguished from the zone below by significant percentages of *Parrotia persica*, *Pterocarya* and Urticaceae–Moraceae and *Gloeotrichia*, a slight drop of Poaceae and a clear maximum of CS waters indicators (13%).

4.2.4. Chronology

A leaf and a rootlet sample from facies Sz2 at 130.5 and 128 cm were taken for radiocarbon dating (Table 1). The raw age for the leaf sample at 130.5 cm is 88 ± 31 BP. Its calibrated age at 95.4% probability (2 sigma) shows two possible ages: AD 1807–1928 (72.6%) and 1684–1732 (27.4%). The median age is AD 1842. The raw age for the rootlet sample at 128 cm is 82 ± 27 BP. Its calibrated age at 95.4% probability (2 sigma) shows two possible ages: AD 1810–1922 (74%) and 1691–1729 (26%). The median age is AD 1847.

Table 1
Radiocarbon dates from Klaus Lagoon (AL11V3 sequence). Calibrated ages are reported for 2σ range with highest probabilities shown in parentheses. Dates from Queen's University of Belfast.

Laboratory number	Sample ID	Depth (cm)	Material type	^{14}C Age (yr BP)	Calibrated age (yr AD) (2σ range)	Median probability
UBA-22991	AL11V3-2-41	128	rootlet	82 ± 27	1810–1922 (74.1%) 1691–1729 (25.9%)	1847
UBA-29891	AL11V3-2-43–44	131–130	leaf	88 ± 31	1807–1928(72.6%) 1684–1732 (27.4%)	1842

5. Discussion

5.1. Amirkola Lagoon

5.1.1. Source of the sediments

Previous studies have suggested that the Amirkola Lagoon was formed by littoral drift of sediments supplied by the Old Sefidrud during a high stand in the LIA (around AD 1600) (Kroonenberg et al., 2000; Lahijani et al., 2009; Leroy et al., 2011; Naderi Beni et al., 2013b). Based on the radiocarbon dating on core HCGL02 taken from the side of the lagoon (Leroy et al., 2011), the age of Amirkola Lagoon at 63 cm depth was estimated at AD1750, and as a result sedimentation rate for this core was estimated at ~ 3.1 mm/y. However, this dating was performed on a sample in the middle of the lagoonal deposits in this coastal core (e.g. 63 cm depth in Fig. 9), and not at the base of the lagoonal deposits (e.g. 80 cm in Fig. 9). Considering the estimated sedimentation rate, the age of lagoon initiation was suggested to be not older than AD 1700. Two sediment sources have been proposed by these authors, viz., river supply of the Old Sefidrud and littoral drift. The results of this study, confirming previous studies, indicate that the sandy layer (sandy silt and silty sand) at the bottom of the sequences represent sand barrier deposition. High MS in these sediments is a result of transport of heavy minerals by the Old Sefidrud and re-deposition and concentration of the sediments by littoral drift and finally formation of barrier. Moreover, these sediments contain *C. glaucum*

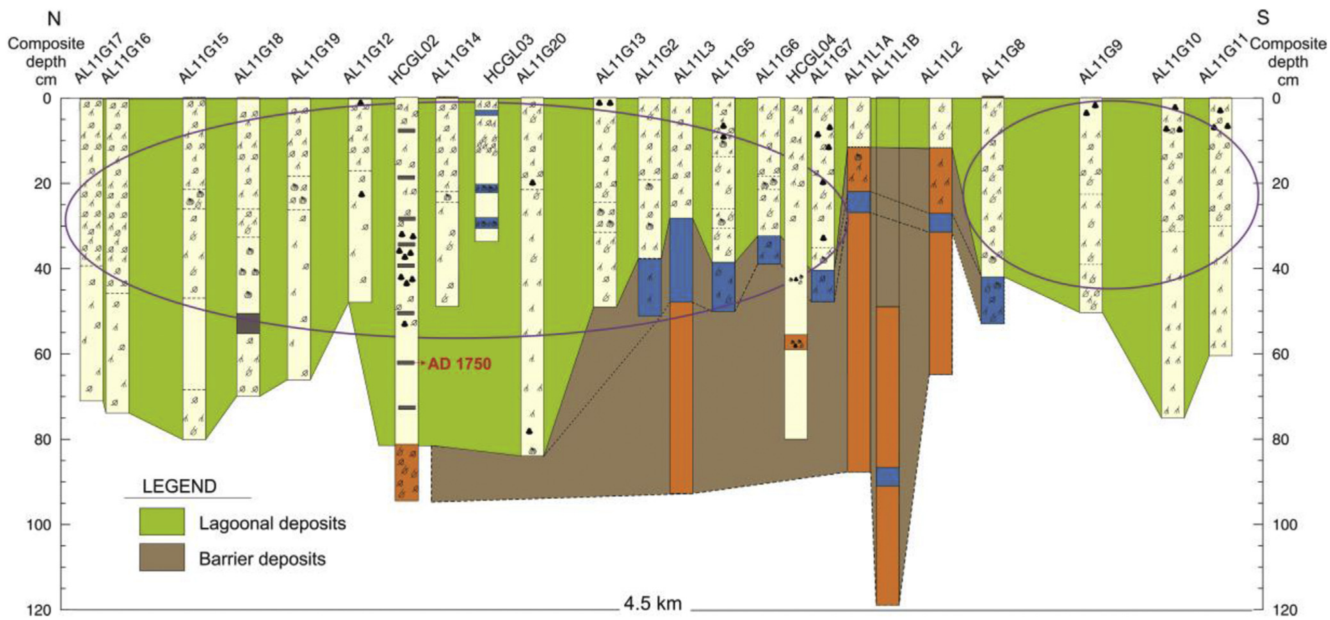

Fig. 9. Correlation of cores in Amirkola Lagoon (For legend of sequences see Fig. 3 and for the core locations see Fig. 1C). Cores HCGL02, HCGL03 and HCGL04 from Leroy et al. (2011).

shells that can live in the open Caspian Sea, and in brackish lagoons. The same layer of silty sand with Caspian shells was recognised at the bottom of core HCGL02 (see Figs. 5 and 6 in Leroy et al. (2011) and Fig. 1C for the location). This coastal core (HCGL02) shows a similar upward increase of OM and $CaCO_3$ as the core AL11G5 located in a deeper part of the lagoon (Fig. 4 A). However, the OM in HCGL02 reaches 40%, while in this study and Lahijani et al. (2009) the amount of OM is up to 10%, due to its shallower location. The present study shows that the horizontal extent of the basal silty sand layer is from the north to the west (Fig. 9).

The top silt layer contains *Ecrobia grimmi*, indeterminate lymnaeaid snails, *Theodoxus pallasi* and charophyte oogenia which indicates a either a very low saline lagoonal environment, or a lagoon with proximal fresh water input. The presence of brackish bivalves (*C. glaucum*) in the lagoonal sediments is due to its connection to the CS in the past (Leroy et al., 2011).

The results also show that the lagoonal sediments are thinner in the centre of lagoon and becoming thicker towards the north and the south (Fig. 9). Possibly the Amirkola Lagoon initiated as two separated lagoons, that eventually became connected (Fig. 9).

5.2. Klaus Lagoon

5.2.1. Vegetation

The vegetation of Pz1 is in a location close to an alder swamp under frequent influence from CS waters. In Pz2 and Pz3, the alder swamp locally disappeared. In a large part of Pz2 from 133 to 70 cm, the environment is isolated from the sea, but CS influence resumes at the top of Pz2 and in Pz3. Diverse signs of agriculture are found: *Diospyros*, *Juglans*, *Olea*, *Vitis*, *Cerealia*-t (most likely rice), Plantaginaceae, *Rumex*, *Polygonum aviculare-bistorta*-t. and Urticaceae–Moraceae (nettles or mulberry). Additionally the dinocyst assemblage is not dominated by *L. machaerophorum*, therefore is likely to pre-date the late 1960s rise in this phytoplankton (see Leroy et al., 2013).

5.2.2. Depositional environment

Different zones, including Sz, Mz and Pz based on different proxies (sedimentology, macro-remains and palynology, respectively), were combined (Fig. 10). Clearly different types of sedimentary environments can be distinguished, reflecting terrestrial, fresh water and brackish conditions. These sub-environments from the bottom to the top include the following.

Facies I: floodplain (281–131 cm)

The facies contains dark brown sand that infers a high-energy environment. It has high MS values (up to 30), indicating an inland source for the sediments. The presence of plant material in the middle part (170–160 cm) appears to confirm the terrestrial origin. Caspian biota are absent in this facies that are therefore interpreted as fluvial sediments, deposited by the Old Sefidrud. This facies is probably not directly deposited in the river channel itself, but under a strong river influence, such as in a floodplain environment, or washover fan.

Facies II: lagoon under frequent brackish water influence (131–119 cm)

This facies consists of olive to olive-grey fine silts and fine sandy sediments, rich in organic matter (up to 3%) with a rich fossil component consisting of numerous gastropod shells (*T. pallasi* and *E. grimmi*), bivalves (*D. polymorpha* and larval shells), charophytes, foraminifers (mainly *A. beccarii* and some *E. brotzkajae*) and dinocysts. This unit is interpreted as a lagoon environment that is under frequent brackish water influence. Indeed, the presence of charophytes and gastropod shells confirm that these facies was deposited in an environment of mixed influences. Presence of foraminifers and dinocysts is an evidence of brackish water invasion from the CS.

Facies III: lagoon protected from the Caspian Sea (119–73 cm)

Above the lagoonal and brackish deposits (facies II), the third unit consists of fine silt and fine sandy sediments, rich in organic matter, with considerable amounts of fungal spores and terrestrial plants, indicating that the lagoon at times was cut off from the CS. Although this unit is interpreted as mostly a closed lagoonal

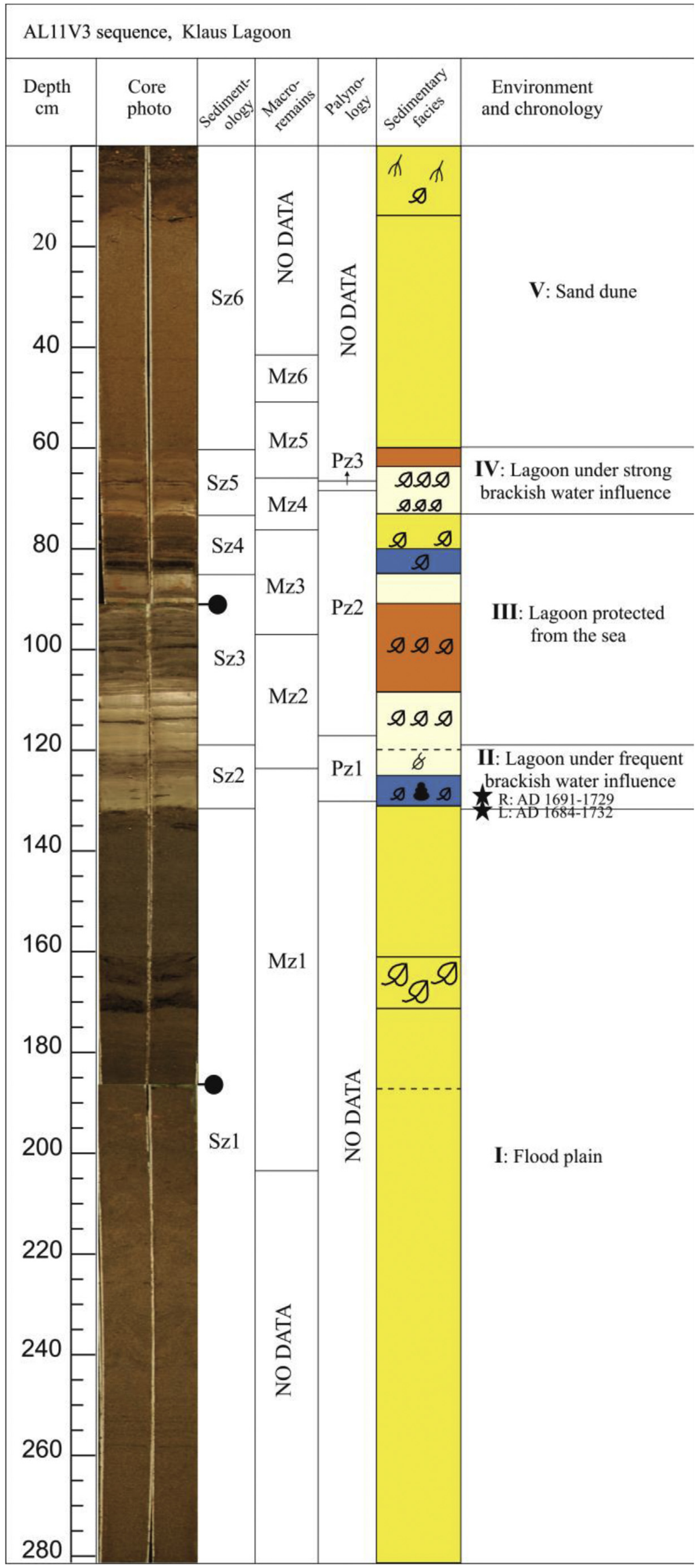

Fig. 10. Comparison of different zones, including sedimentology, macro-remains and palynology, and depositional environments in sequence AL11V3, for Klaus Lagoon (For legend see Fig. 5), black stars: location of radiocarbon dates, R: rootlet (materials dated).

environment, a minor Caspian invasion (as shown by the presence of dinocysts and foraminifers) occurred.

Facies IV: lagoon under strong brackish water influence (73–60 cm)

Fine brown silty sediment, rich in OM, is considered as deposited in an open lagoonal environment because of the abundance of foraminifers (*A. beccarii* and *E. brotzkajae*), bivalve shells and dinocysts.

Facies V: sand dune and modern soil (60–0 cm)

The fifth facies consists of dark yellowish brown sand deposits with relatively high MS (up to 28). This facies is interpreted as sand dune, covered by soil at the top. The top of facies V is 2.61 m above the present level of the CS in 2015.

5.2.3. Age calibration of Klaus Lagoon

Two dates were obtained on the bottommost part of facies II: they show practically identical ages (Table 1). The explanation provided here is based on the sample at 130.5 cm, which represent the beginning of deposition of lagoonal deposits. This dating provides two possible ages: AD 1807–1928 with 72.6% probability and AD 1684–1732 with 27.4% probability (Table 1). During the period of AD 1807–1928 the water level was relatively constant with minor fluctuations less than 1 m. Therefore, the second probability (i.e. AD 1684–1732), and more likely after AD 1715 (start of a water-level rise), is used for the interpretation of the sequence. At the same time, Amirkola Lagoon was formed in c. AD 1700 (Leroy et al., 2011) under rapid CS level rise. The formation of sand barriers and back-barrier lagoons along the western Caspian coast in Dagestan are discussed in Kroonenberg et al. (2007). In Klaus Lagoon, the lagoon formation happened at the same time as the Amirkola Lagoon formation and slightly after the Turali Lagoon formation in Dagestan (i.e. AD 1628). The Klaus Lagoon was under the brackish water invasion (facies II in Fig. 10) and became separated from the CS (facies III in Fig. 10).

5.2.4. Evolution of the Klaus coastal lagoon through time and related water levels

Prior to the avulsion currently dated around AD 1600, the main distributary was the Old Sefidrud. Its outflow brought a large volume of sediment and it can reasonably be assumed that the delta was further advanced north-eastward than at present.

In the first stage (stage A in Fig. 11), between AD 1715 and AD 1805, the CS level rose up to −23.8 m (the water level rise between AD 1715–1805 (Brückner, 1890; Leroy et al., 2011; Naderi Beni et al., 2013a) and Klaus Lagoon formed behind a sand barrier. At this stage, either a connection with the CS remained or salinity was not lowered by run-off or ground water input as judged from the abundance of brackish water species. Therefore, the lagoon formed a suitable environment for brackish water species.

The rapid CS level fall between AD 1805 and 1875 when the CS level reached −25 m in AD 1875 caused a seaward shift (stage B in Fig. 11). Meanwhile, the area was subjected to intensive erosion as a result of abrupt reduction of sediment supply from the Old Sefidrud due to river avulsion. Erosion has increased since the avulsion along this section of the coast (west of the Sefidrud). Recent evidence of erosion suggests that landward shift of the coast is happening in this area since AD 1978 in

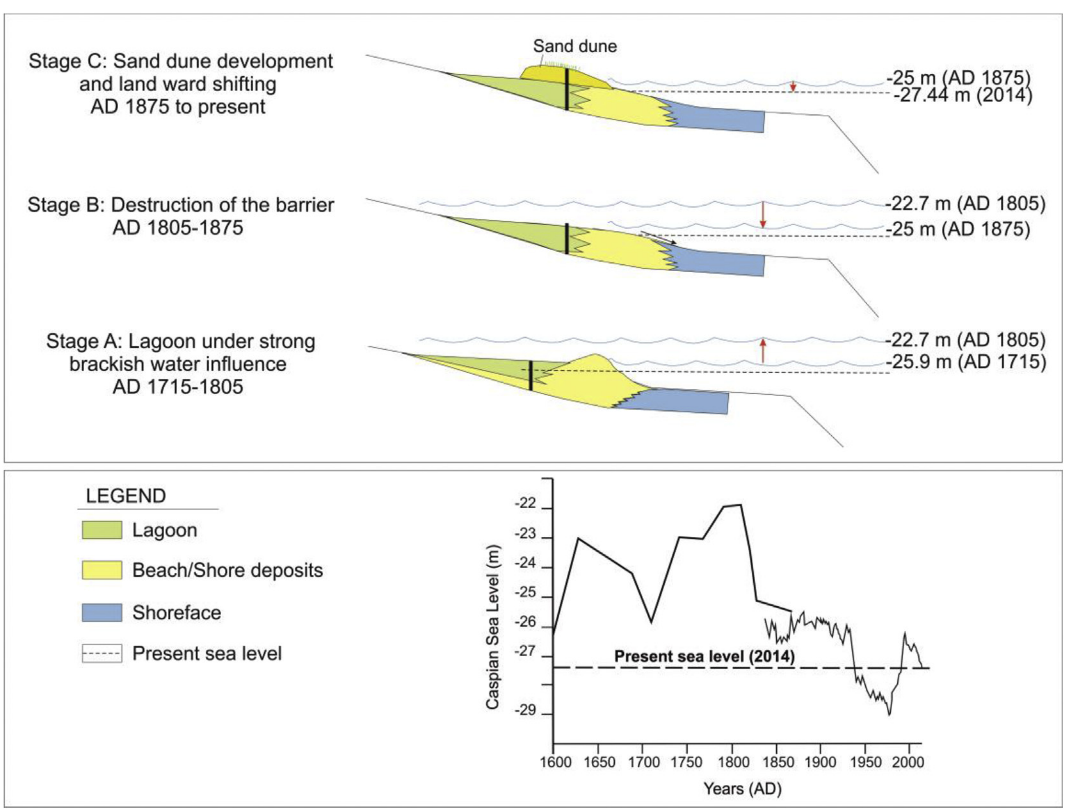

Fig. 11. Evolution of Klaus Lagoon through time and related sea levels (dates from the sea level curve of Naderi Beni et al. (2013a)).

response to rapid CS level rise (Kakroodi et al., 2012). According these authors, the rate of regression during 1978–2000 in this area was 181 m/y. Regressions with rate of 60–100 and 150–200 m/yr were also recorded in the north-eastern and north-western of CS, during the rapid CS level fall (Ignatov et al., 1993; Kaplin and Selivanov, 1995). However, wind still remains a source of sediment deposition in this area and sand dunes can develop along the coast (stage C in Fig. 11). Lahijani et al. (2009) and Kazancı et al. (2004) have discussed the possibility of coastal sand deposition in form of sand dune in the Sefidrud Delta. Sand dune formation was also observed in the field along the coastal line in the area between Anzali and Zibakenar Lagoons in 2011.

5.3. *Different response of two lagoons on two sides of the Old Sefidrud*

Coastal erosion is most likely to occur in coastal lowland areas and along soft sediment coastlines. Relative sea level rise and a shortage of sand supply are the most widely publicised causes of the erosion. However, morphology of the coastline plays a major role in the rate of erosion. In the study area, the sharp corner of coastline at the east of Old Sefidrud decreases wave energy. Therefore the NW–SE coastline east of Amirkola Lagoon has not been subjected to high erosion. However, waves and wave induced currents have had a major impact on morphology of coastline oriented west-east in this part of the delta. The Klaus Lagoon is in an area of high erosion (coastline oriented W–E), yet the Amirkola Lagoon with its N–S oriented coastline is not susceptible to erosion. Consequently, the rate of coastal erosion is different on each side of the Old Sefidrud. Moreover, the results show that the west-east coast of the delta was more advanced to the north (as a barrier system was required to allow the development of Klaus lagoon). The Old Sefidrud had lagoons on its both sides which is similar to the present new Sefidrud.

6. Conclusions

In the early eighteenth century, Klaus Lagoon and Amirkola Lagoon came into existence on the two sides of the Old Sefidrud mouth, as a response to rapid CS-level rise. The Old Sefidrud delta became subject to erosion due to rapid sea level rise and reduction of sediment supply caused by river avulsion. This has continued during the last rapid CS level rise between 1977 and 1995. However, different sides of the river delta show a different rate of erosion/accumulation due to the eastward direction of the long-shore current.

Acknowledgements

This research is part of the PhD of the first author entitled “Evaluation of Sefidrud Delta (South West Caspian Sea) during the last millennium”, which was funded by Brunel University London. The publication is a contribution to the INQUA QuickLakeH project (No 1227) and to the European project Marie Curie, CLIMSEAS–PIRSES–GA–2009–247512. Iranian National Institute for Oceanography and Atmospheric Science (INIOAS) is especially thanked for organising the field campaign and measuring the elevation of the Klaus Lagoon.

Appendix A

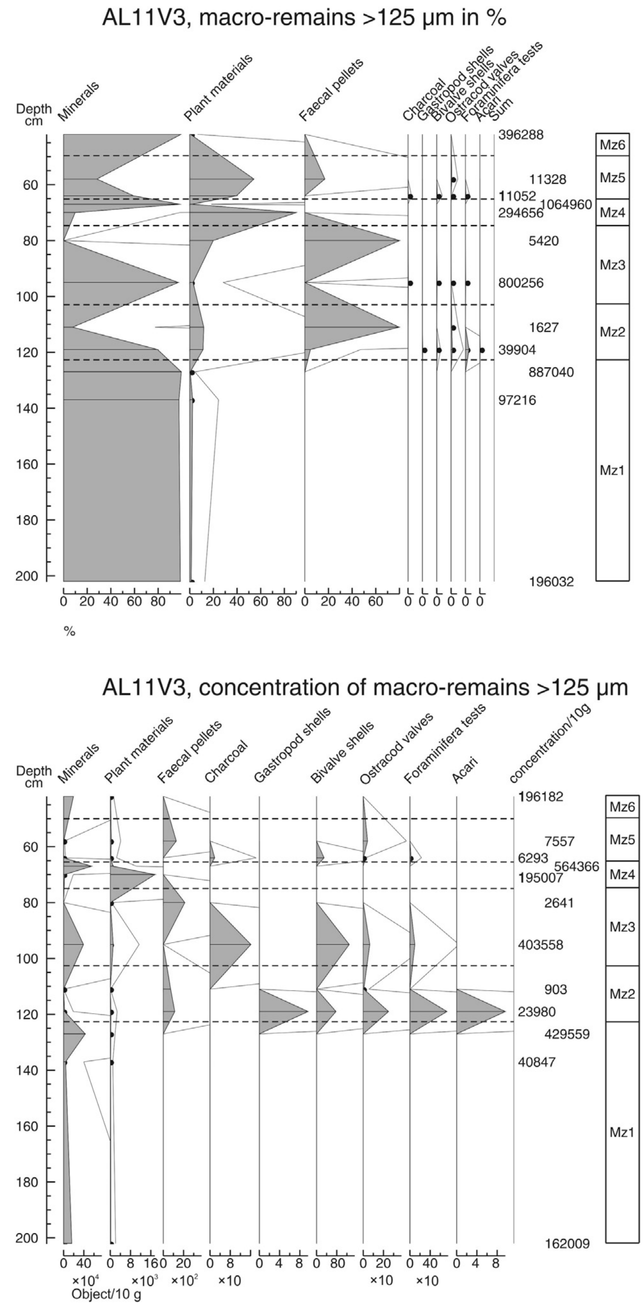

Fig. A1. Percentages of macro-remains above 125 µm (the diagram at the top) and concentrations (the diagram at the bottom) in the sequence AL11V3 (including Klaus Lagoon). Black dots represent values lower than 0.05% in percentage graph and 5 objects in concentration graph.

References

Bennett, K., 2007. Psimpoll and Pscomb Programs for Plotting and Analysis. Version 4.27. www.chrono.qub.ac.uk/psimpoll/psimpoll.html (last accessed 16.01.15.).

Birks, H.H., 2001. Plant macrofossils. In: Smol, J.P., Birks, H.J.B., Last, W.M. (Eds.), Tracking Environmental Change Using Lake Sediments. Springer, Netherlands, pp. 49–74.

Blott, S.J., Pye, K., 2001. GRADISTAT: a grain size distribution and statistics package for the analysis of unconsolidated sediments. Earth Surface Processes and Landforms 26 (11), 1237–1248.
Brückner, E., 1890. Climate Fluctuations since 1700, along with Comments about the Climatic Fluctuations of the Diluvial Period. Vienna: E. Holzel (in German).
Folk, R.L., 1974. Petrology of Sedimentary Rocks (Hemphill, Texas).
Haghani, S., Leroy, S., Khdir, S., Kabiri, K., Naderi Beni, M., Lahijani, H.A.K., 2015. An early Little Ice Age brackish water invasion along the south coast of the Caspian Sea (sediment of Langarud wetland) and its wider impacts on environment and people. The Holocene in press (accepted May 2015). Published online before print July 24, 2015, doi:10.1177/0959683615596835 Link: http://hol.sagepub.com/content/early/2015/07/24/0959683615596835.refs.
Heiri, O., Lotter, A.F., Lemcke, G., 2001. Loss on ignition as a method for estimating organic and carbonate content in sediments: reproducibility and comparability of results. Journal of Paleolimnology 25 (1), 101–110.
Ignatov, Y.I., Kaplin, P.A., Lukyanova, S.A., Solovieva, G.D., 1993. Evolution of the Caspian Sea coasts under conditions of sea-level rise: model for coastal change under increasing "greenhouse effect". Journal of Coastal Research 104–111.
Kakroodi, A.A., Kroonenberg, S.B., Hoogendoorn, R.M., Mohammd Khani, H., Yamani, M., Ghassemi, M.R., Lahijani, H.A.K., 2012. Rapid Holocene sea-level changes along the Iranian Caspian coast. Quaternary International 263, 93–103.
Kaplin, P., Selivanov, A., Lukyanova, S., 2010. Azerbaijan. In: Bird, E. (Ed.), Encyclopedia of the World's Coastal Landforms. Springer Science and Business Media, pp. 885–888.
Kaplin, P.A., Selivanov, A.O., 1995. Recent coastal evolution of the Caspian Sea as a natural model for coastal responses to the possible acceleration of global sea–level rise. Marine Geology 124 (1), 161–175.
Kazancı, N., Gulbabazadeh, T., 2013. Sefidrud Delta and Quaternary Evolution of the Southern Caspian.
Kazancı, N., Gulbabazadeh, T., Leroy, S.A., Ileri, ö., 2004. Sedimentary and environmental characteristics of the Gilan–Mazenderan plain, northern Iran: influence of long-and short-term Caspian water level fluctuations on geomorphology. Journal of Marine Systems 46 (1), 145–168.
Kousari, S., 1986. Evolution of Sefidrud Delta. Development in Geological Education 1, 31–41 (in Persian).
Krasnozhon, G.F., Lahijani, H., Voropayev, G.V., 1999. Evolution of the delta of the Sefidrud River, Iranian Caspian Sea coast, from space imagery. Mapping Science and Remote Sensing 36, 256–264.
Kroonenberg, S.B., Abdurakhmanov, G.M., Badyukova, E.N., Borg, K.V.D., Kalashnikov, A., Kasimov, N.S., Rychagov, G.I., Svitoch, A.A., Vonhof, H.B., Wesselingh, F.P., 2007. Solar–forced 2600 BP and little Ice Age highstands of the Caspian Sea. Quaternary International 173, 137–143.
Kroonenberg, S., Badyukova, E., Storms, J., Ignatov, E., Kasimov, N., 2000. A full sea–level cycle in 65years: barrier dynamics along Caspian shores. Sedimentary Geology 134 (3), 257–274.
Lahijani, H.A.K., Rahimpour–Bonab, H., Tavakoli, V., Hosseindoost, M., 2009. Evidence for late Holocene highstands in central Guilan–East Mazanderan, south Caspian coast, Iran. Quaternary International 197 (1), 55–71.
Lahijani, H.A.K., Tavakoli, V., Amini, A.H., 2008. South Caspian river mouth configuration under human impact and sea level fluctuations. Environmental Sciences 5, 65–86.
Leroy, S.A.G., 2010. Palaeoenvironmental and palaeoclimatic changes in the Caspian Sea region since the Lateglacial from palynological analyses of marine sediment cores. Geography, Environment, Sustainability 2, 32–41. Faculty of Geography of Lomonosov Moscow State University and by the Institute of Geography of RAS. http://www.geogr.msu.ru/GESJournal/ (last accessed 30.06.15.).
Leroy, S., Lahijani, H., Reyss, J., Chalié, F., Haghani, S., Shah–Hosseini, M., Shahkarami, S., Tudryn, A., Arpe, K., Habibi, P., 2013. A two–step expansion of the dinocyst *Lingulodinium machaerophorum* in the Caspian Sea: the role of changing environment. Quaternary Science Reviews 77, 31–45.
Leroy, S., Marret, F., Giralt, S., Bulatov, S., 2006. Natural and anthropogenic rapid changes in the Kara–Bogaz Gol over the last two centuries reconstructed from palynological analyses and a comparison to instrumental records. Quaternary International 150 (1), 52–70.
Leroy, S.A.G., Tavakoli, V., Habibi, P., Naderi Beni, M., Lahijani, H.A.K., Djamali, M., Naqinezhad, A., Moghadam, M.V., Arpe, K., Shah–Hosseini, M., Hosseindoust, M., Miller, C.S., 2011. Late little Ice Age palaeoenvironmental records from the Anzali and Amirkola lagoons (south Caspian Sea): vegetation and sea level changes. Palaeogeography, Palaeoclimatology, Palaeoecology 302 (3), 415–434.
Mann, M.E., Zhang, Z., Rutherford, S., Bradley, R.S., Hughes, M.K., Shindell, D., Ammann, C., Faluvegi, G., Ni, F., 2009. Global Signatures and dynamical origins of the little Ice Age and medieval climate anomaly. Science 326, 1256–1260.
Marret, F., Leroy, S.A.G., Chalié, F., Gasse, F., 2004. New organic–walled dinoflagellate cysts from recent sediments of Central Asian seas. Review of Palaeobotany and Palynology 129 (1), 1–20.
Mazzullo, J.M., Meyer, A., Kidd, R., 1988. New sediment classification scheme for the ocean drilling program. In: Mazzullo, J.M., Graham, A.G. (Eds.), Handbook for Shipboard Sedimentologists, ODP Technical Notes 8, pp. 45–67.
Molavi–Arabshahi, M., Arpe, K., Leroy, S.A.G., 2015. Precipitation and temperature of the Southwest Caspian Sea during the last 56 years, their trends and teleconnections with large–scale atmospheric phenomena. International Journal of Climatology accepted with minor changes. in press (accepted June 2015). Published online in Wiley Online Library (wileyonlinelibrary.com), doi:10.1002/joc.4483. link: http://onlinelibrary.wiley.com/doi/10.1002/joc.4483/full.
Naderi Beni, A., Lahijani, H.A.K., Harami, R.M., Arpe, K., Leroy, S.A.G., Marriner, N., Berberian, M., Andrieu–Ponel, V., Djamali, M., Mahboubi, A., 2013a. Caspian Sea level changes during the last millennium: historical and geological evidences from the south Caspian Sea. Climate of the Past 9, 1645–1665.
Naderi Beni, A., Lahijani, H., Harami, R.M., Leroy, S.A.G., Shah–Hosseini, M., Kabiri, K., Tavakoli, V., 2013b. Development of spit–lagoon complexes in response to Little Ice Age rapid sea–level changes in the central Guilan coast, South Caspian Sea, Iran. Geomorphology 187, 11–26.
Reimer, P.J., Bard, E., Bayliss, A., Beck, J.W., Blackwell, P.G., Ramsey, C.B., Buck, C.E., Cheng, H., Edwards, R.L., Friedrich, M., Grootes, P.M., Guilderson, T.P., Haflidason, H., Hajdas, I., Hatté, C., Heaton, T.J., Hoffmann, D.L., Hogg, A.G., Hughen, K.A., Kaiser, K.A., Kromer, B., Manning, S.W., Niu, M., Reimer, R.W., Richards, D.A., Scott, E.M., Southon, J.R., Staff, R.A., Turney, C.S.M., Plicht, J.V.D., 2013. IntCal13 and Marine13 radiocarbon age calibration curves 0–50,000 years cal BP. Radiocarbon 55 (4), 1869–1887.
Ruddiman, W.F., 2008. Earth Climate, Past and Future. W. H. Freeman and Company, New York.
Stuiver, M., Reimer, P.J., 1993. Extended ^{14}C database and revised Calib 3.0 ^{14}C age calibration program. Radiocarbon 35, 215–230.